

Electronic structure of Ag-adsorbed nanowire-like stripes on Si(110)-(16×2) surfaces.

I. An *in situ* STM and STS experiment

K. Bhattacharjee,¹ A. Roy,¹ K. Kundu,^{1,2} and B. N. Dev^{1,3,*}¹*Institute of Physics, Sachivalaya Marg, Bhubaneswar 751005, India*²*Visva-Bharati, Santiniketan 731 235, West Bengal, India*³*Department of Materials Science, Indian Association for the Cultivation of Science,**2A & 2B Raja S. C. Mullick Road, Jadavpur, Kolkata 700032, India*

(Received 4 September 2007; published 18 March 2008)

The surface morphology and electronic structure of an ultrathin Ag film ($\frac{1}{8}$ monolayer) deposited under ultrahigh vacuum condition on Si(110)-(16×2) surfaces was studied by *in situ* scanning tunneling microscopy and scanning tunneling spectroscopy (STS). Local density of states, obtained from our STS data, reveal that after Ag deposition, the band gap of the surface has increased compared to the bulk Si band gap of 1.1 eV. In addition, the band offset and appearance of new electronic states within the band gap are observed. We have made an attempt to understand these results by a one-dimensional (1D) tight binding model calculation by considering various modified chains. In the theoretical analysis of the model, real space renormalization technique and Green's function approach are adopted. The results obtained from the 1D model qualitatively explain the observed features in the local density of states.

DOI: [10.1103/PhysRevB.77.115430](https://doi.org/10.1103/PhysRevB.77.115430)

PACS number(s): 68.35.B-, 73.20.-r, 68.37.Ef

I. INTRODUCTION

Among the low-index nonvicinal surfaces of Si, such as Si(111), Si(100), and Si(110) surfaces, only the Si(110) surface with a particular surface reconstruction, namely, (16×2) reconstruction, shows a nanowirelike structure. The (16×2) reconstructed Si(110) surface consists of equally spaced and alternately raised and lowered stripes lying along the $[\bar{1}12]$ direction. The spacing between the adjacent raised stripes is about 5 nm and the width of a stripe is about 2 nm. Considering these features, the stripes on the Si(110)-(16×2) reconstructed surface may be assumed to represent a quasi-one-dimensional system. Adsorption of some elements on the stripes of the (16×2) reconstructed Si(110) surface and the evolution of the electronic structure would be interesting to investigate. Ag on Si surfaces have been classically treated as an ideal system to study various aspects in surface science. Thus, it would be worthwhile to study Ag adsorption on the nanowire-like stripes on the Si(110)-(16×2) surfaces. We investigate the electronic structure of this system by scanning tunneling spectroscopy experiments. As such, it is difficult to produce the (16×2) reconstructed surface of Si(110).^{1,2} It is even more difficult to prepare a large (16×2) reconstructed area. In this case, a microspectroscopic technique such as scanning tunneling spectroscopy (STS) is suitable for the study of the electronic structure of this surface.

In order to understand the results of our experiment, we present a one-dimensional (1D) tight binding model calculation using Green's function formalism.³ Since we are interested in explaining, among other results, the band gap broadening, we primarily consider a periodic system.⁴

Among the low-index surfaces of silicon, Si(110) surface is not yet properly understood. It has been observed that Si(110) surface can give a wide variety of atomic reconstruc-

tions $[(2 \times 1), (5 \times 1), [4(5) \times 5(4)], [7(9) \times 1], (16 \times 2), (32 \times 2)]$ after cleaning, among which (16×2) and (5×1) are considered to be the two primary reconstructed surfaces. A contaminant-free, nonvicinal and well annealed Si(110) surface exhibits (16×2) reconstruction,⁵⁻⁸ whereas the presence of a very slight amount of impurity such as Ni can destroy this surface reconstruction and can show a smaller unit cell reconstruction of the (5×1) surface^{5,9,10} or forming various other reconstructions which are mostly Ni induced.^{11,12}

On the study of the Si(110)-(16×2) surface, there are only a few reports available in the literature. There are even fewer studies on adsorption on this surface. Due to the experimental difficulties on the surface preparation, the electronic properties of the clean Si(110)-(16×2) phase are scarcely known and there are only a couple of photoemission studies available.^{13,14} Several scanning tunneling microscopy (STM) studies on the (16×2) surfaces show that this phase only partly covers the surface. In this situation, a microspectroscopic technique such as STS is ideally used for the study of electronic structure, so that electronic structure can be studied on the relevant portion of the surface. That is why we have chosen the STS technique to study Si(110)-(16×2) and the Ag-adsorbed (16×2) surfaces. Structural details of a Si(110) surface have been obtained from STM measurements which revealed that the reconstructed Si(110)-(16×2) surface consists of equally spaced and alternately raised and lowered "upstripes" and "downstripes" parallel to the $[\bar{1}12]$ direction which are separated by atomic steps of height $a_0/2\sqrt{2}$, where a_0 is the bulk lattice constant. The stripes consist of a zigzag pattern with a repetition distance of $\sqrt{6}a_0$.¹⁵ The stripes are stacks of paired elements, the shape of which is interpreted differently by various authors as octets,¹⁰ pentagons,⁸ or centered stretched hexagons.¹⁵ It has been observed that the (16×2) reconstruction occurs in two

domains with the step boundaries along the $[\bar{1}12]$ or the $[1\bar{1}2]$ direction where both domains form a periodic up and down sequence of terraces with a height difference of about one Si(110) bulk layer spacing (~ 0.19 nm). According to the centered stretched hexagon model,¹⁵ the surface unit cell lattice vectors (a', b') of the (16×2) reconstruction is not actually $16a$ and $2b$ [a and b being unit cell vectors on an ideal Si(110) surface] but follows, the

$$\begin{pmatrix} -1 & 17 \\ 2 & -2 \end{pmatrix}$$

structure [that is, $a' = -a + 17b$ and $b' = 2a - 2b$]. However, other authors⁵⁻⁸ have given a

$$\begin{pmatrix} 11 & -5 \\ 2 & 2 \end{pmatrix}$$

notation for the 16×2 reconstructed surface. Within the centered stretched hexagon model structure, the distance between two consecutive upstripes or two consecutive downstripes was found to be 5.02 nm and the repeat distance of the zigzag pattern is 1.33 nm. It has been observed that most of the times the (16×2) reconstruction forms a stripe-and-chevron structure where the stripes are directed towards the $[\bar{1}12]$ direction and the chevron is directed towards the $[1\bar{1}2]$ direction. Chevron structure makes an angle of 70.5° with the stripes. Energetically, the (16×2) surface reconstruction is favorable.^{15,16}

There are several reports of STM studies which reveal the formation of (16×2) and (5×1) phases and various models have been introduced to understand their atomic structures,^{8,10,15} especially the atomic arrangement of the (16×2) reconstruction and the total energy calculations were performed.¹⁶ However, so far, there is no well-accepted structural model for the (16×2) reconstructed surface. In the present study, we investigate the electronic structures of (i) a bare 16×2 surface and (ii) a Ag-adsorbed 16×2 surface by *in situ* STS. STS measurements were made by placing the STM tip over various points on the 16×2 structures. Local density of states (LDOS) reveal an electronic band gap of around 1.1 eV, which corresponds to the bulk Si band gap. We have deposited an ultrathin Ag layer [$\frac{1}{8}$ monolayer (ML)] on this 16×2 structure in a molecular beam epitaxy system with the substrate at room temperature [1 ML = 0.96×10^{15} atoms/cm², or the atomic density on an ideal Si(110) surface]. After Ag deposition, the surface was again characterized by *in situ* STM and STS measurements. STS spectra now taken at different points on the wirelike structures of Ag-adsorbed (16×2) surfaces show that the band gap of the surface has increased compared to the bulk Si band gap of 1.1 eV. We attempt to understand the observations, namely, (i) band gap broadening, (ii) band gap variation, (iii) band offset, and (iv) appearance of new electronic states within the band gap, by a one-dimensional tight binding model calculation using Green's function formalism.

II. EXPERIMENTAL DETAILS

Experiments were carried out in a custom built ultrahigh vacuum chamber (UHV) where the base pressure inside the growth chamber remains of the order of low 10^{-10} mbar to high 10^{-11} mbar. The base pressure inside the growth chamber during this experiment was 1.7×10^{-10} mbar. The UHV chamber is fitted with a reflection high energy electron diffraction system and is attached with a UHV variable temperature scanning tunneling microscope (from Omicron Nanotechnology, Germany) for postgrowth characterization of the samples. This system has been described elsewhere.¹⁷ P-doped *n*-Si(110) (oriented within $\pm 0.5^\circ$) with resistivity of 5–20 Ω cm was loaded in the growth chamber. Atomically clean, reconstructed Si(110)- (16×2) surface was prepared by usual heating and flashing procedure. The samples were first degassed at about 600 $^\circ$ C for 12–14 h followed by a flashing at ~ 1200 $^\circ$ C for 2–3 min. Then, the sample was cooled down to RT and it was transferred *in situ* into the STM chamber for STM and STS measurements. STM measurements confirm the formation of the (16×2) phase along the step edges and on the terraces. STM measurements also reveal the formation of other mixed phases on the surface coexisting with the (16×2) structures. We concentrate only on the (16×2) reconstruction in the present work. STM images reveal the usual stripe and chevron structures of the (16×2) reconstruction. STS data were taken on the 16×2 stripes and chevron structures at different points. After the STM and STS measurements were carried out on the Si(110)- (16×2) surface, the sample was transferred to the growth chamber for Ag deposition. An ultrathin layer of Ag ($\frac{1}{8}$ ML) was deposited at room temperature (RT) from a Knudsen cell with a PBN (pyrolytic boron nitride) crucible. The postgrowth investigations of the surface morphology and the electronic structure of the surface were again carried out by STM and STS measurements. After the postgrowth characterizations were made, the sample was again transferred to the growth chamber and flashed at ~ 1200 $^\circ$ C for 2–3 min in order to desorb Ag. STM measurements now show Si(110)- (5×1) atomic reconstruction, which prevails all over the surface, including the areas of mixed phases, which existed surrounding the (16×2) phase; no (16×2) reconstruction was observed. This is consistent with previous observations that the presence of minute contamination leads to an absence of (16×2) reconstruction and usually a (5×1) reconstruction appears.¹⁵

III. RESULTS AND DISCUSSIONS

STM images of a clean Si(110)- (16×2) surface with stripes and chevron structures are shown in Figs. 1(a)–1(e). The stripe pattern in the STM images with alternate upstripes and downstripes is typical of the (16×2) reconstruction.¹⁵ These structures are observed to form nearly all along the step edges and on the terraces. This (16×2) phase is seen to coexist with other mixed phases surrounding the (16×2) structures. Figures 1(f) and 1(g) are the height profiles taken from the STM images of Figs. 1(d) and 1(e), respectively, along the lines marked on the images. The line profiles show

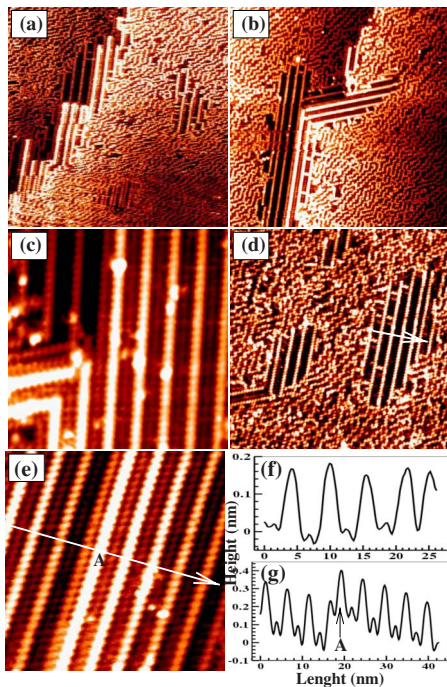


FIG. 1. (Color online) STM images of Si(110)-(16 \times 2) surfaces. Scan size: (a) 150 \times 210 nm², (b) 148 \times 148 nm², (c) 39 \times 40 nm², (d) 107 \times 107 nm², and (e) 40 \times 40 nm². All these images are taken at bias voltage $V_s=2.1$ V and tunneling current $I=0.2$ nA. (f) and (g) are the height profiles taken along the lines marked in (d) and (e), respectively. Note here that the scales are different for (f) and (g). Note that the upstrips at A and to its right side are higher by ~ 0.2 nm compared to those on the left side of A indicating the presence of two adjacent terraces separated by a step of monatomic height at A.

the upstrips and downstrips of the (16 \times 2) structure. The distance between two upstrips or downstrips is found to be ~ 5 nm and the height difference between upstripe and downstripe is ~ 0.2 nm [Figs. 1(f) and 1(g)] which corresponds to one-atomic-step height difference between upstrips and downstrips. These results are consistent with previously reported results.¹⁵ Within the width of each upstripe or downstripe, there are three Si atoms.¹⁵ Unfortunately, we could not resolve these atoms individually. A hexagonal arrangement of atoms with a periodicity of ~ 1.3 nm runs along each stripe.¹⁵ Atomic arrangements¹⁵ on the upstrips are shown schematically in Fig. 2. The width of each upstripe observed in our case is found to be ~ 2 nm. We observe the formation of (16 \times 2) phase structures at the step edges as well as on the terraces. On the terraces, as in Fig. 1(d), the downstrips are not visible in the image. However, a height profile taken across the stripe structure, shown in Fig. 1(f), reveals the presence of the lower stripes as well. We show an image of the Ag-deposited surface, along with a line profile, in Fig. 3. If we concentrate on the upstrips in the line profile, we notice that the (16 \times 2) periodicity is partly disturbed upon Ag deposition. Figure 4 shows two images—one from the bare Si(110) surface (a) and another following Ag deposition on this surface (b)—along with their Fourier transformations. The power spectrum image (Fourier

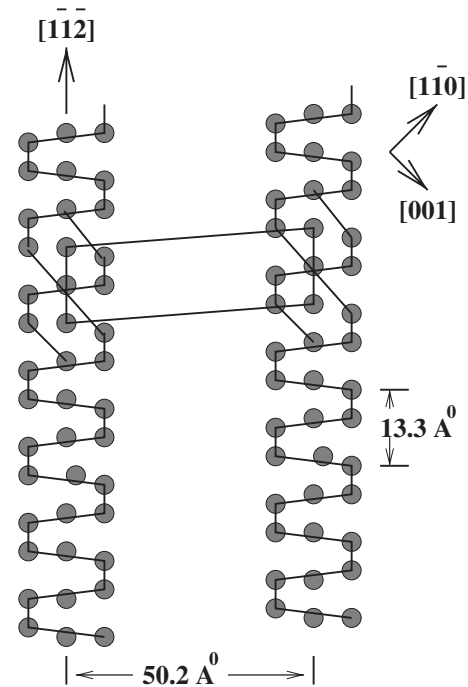


FIG. 2. Schematic representation of two neighboring upstrips of a Si(110)-(16 \times 2) structure. Surface unit cell is marked in the image (see Ref. 15).

transformation) taken from Fig. 4(a) is shown in Fig. 4(c). The periodicities of the (16 \times 2) structure is observed as ordered spots in the Fourier transformed image in Fig. 4(c). Figure 4(d), the Fourier transform of Fig. 4(b), shows a fuzzy (16 \times 2) pattern. Figure 5 shows two additional images from the Ag-adsorbed Si(110) surface. Some points, where STS measurements were made, are marked on the images. In order to understand the electronic structures of these systems, we have used *in situ* STS study to investigate the LDOS associated with these structures. Figure 6 shows the normalized conductance $[(dI/dV)/(I/V)]$ vs V curves which are proportional to the LDOS plotted as a function of bias voltage (V). dI/dV curves are extracted from the I - V data curves obtained at various points on top of the upstrips and downstrips with the usual software programming available which we use for scanning and data analysis. Spectra

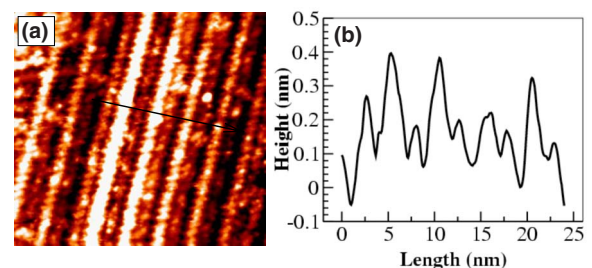


FIG. 3. (Color online) (a) A STM image shows the surface after Ag ($\frac{1}{8}$ ML) deposition. The scan area is 40 \times 40 nm². The stripes are still visible in the image. (b) The line profile taken along the line marked in (a). Line profile now shows a bit irregular pattern.

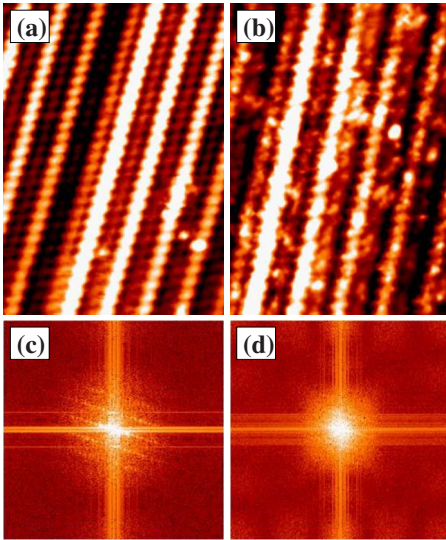


FIG. 4. (Color online) Power spectrum (Fourier transformed images) taken from the STM images of (a) and (b) are shown in (c) and (d), respectively. Image (a) corresponds to a bare Si(110)-(16 \times 2) reconstructed surface and (b) was obtained after Ag deposition. Periodicity of the 16 \times 2 surface (a) before Ag deposition is clearly seen in the Fourier transformed image (c). However, after Ag deposition, we do not observe any new periodicity in the Fourier transformed image as seen from (d); the (16 \times 2) spots are also more fuzzy.

numbered 1 and 2 in Fig. 6 are two typical spectra for the clean Si(110)-(16 \times 2) structures. STS spectra reveal a well-defined band gap of ~ 1.1 eV in the normalized $(dI/dV)/(I/V)$ vs V curves which correspond to the bulk band gap of Si. STS spectra taken at various locations are different in detail. From these spectra, we identify the filled states at energies around -0.5 , -0.7 , -1.0 , -1.3 , -1.7 , and -2.4 eV. Some of these have been observed in the angle resolved photoemission studies.^{13,14} For the empty states, we obtain peak features around 0.6, 0.8, 1.3, 1.5, 1.8, 2.0, and 2.3 eV. Some of these are consistent with the results of surface differential resistivity measurements.^{13,14} In addition, we observe LDOS features within the band gap.

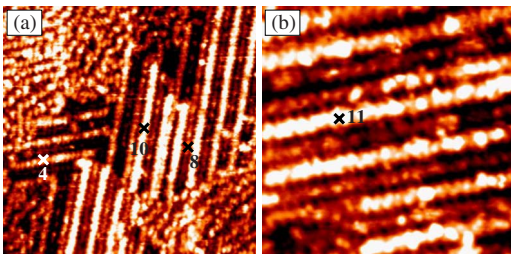


FIG. 5. (Color online) STM images of Si(110)-(16 \times 2) surface after $\frac{1}{8}$ ML Ag deposition. (16 \times 2) structures are still visible. Scan size: (a) 70 \times 70 nm² and (b) 30 \times 27 nm². The points marked in the images as 4, 8, 10, and 11 correspond to the points where the I - V data have been taken to get the $(dI/dV)/(I/V)$ curves 4, 8, 10, and 11, respectively, shown in Fig. 6. Other spectra were obtained in a similar fashion from different STM images, not shown here.

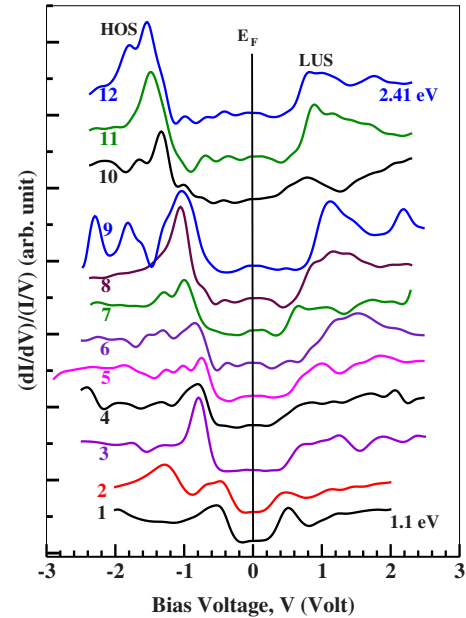


FIG. 6. (Color online) Normalized $(dI/dV)/(I/V)$ vs V spectra taken at different locations on the surface at RT during STM scanning. Each spectrum has been assigned a number on the left side of the figure, whereas the value of the band gap calculated from each of these spectra is written on the right side. Spectra 1 and 2 are taken on the Si(110)-(16 \times 2) surfaces before Ag deposition. These two curves show a band gap around 1.1 eV which is like bulk Si band gap. Spectra 3–12 are taken after $\frac{1}{8}$ ML Ag deposition on Si(110)-(16 \times 2) surfaces. All these spectra show an increase in band gap.

STM images obtained after Ag deposition (Fig. 5) show that the (16 \times 2) structures are still preserved on the surface with upstripes and downstripes. However, the line profiles obtained along these structures (not shown here) show an irregular behavior (which is also observed from the STM images) though stripe structures are also observed in the profiles. After Ag deposition, we do not observe any new periodicity in the Fourier transformed images indicating that Ag deposition has not produced any long-range ordered structure.

We have deposited Ag at a low coverage ($\frac{1}{8}$ ML) to capture the expected large variations in local electronic structure, as STS is the most appropriate technique for capturing a wide variety of local electronic structures. As the dangling bond density is larger than 0.5/atom,¹⁵ $\frac{1}{8}$ ML Ag could saturate only a fraction of them leading to locations with different environments and consequently different electronic structures. We have also addressed these variations in the theoretical model. STS measurements were performed in a similar fashion on Ag-deposited upstripes and downstripes of the (16 \times 2) structures and the normalized conductance curves were obtained. Figure 6 (spectra 3–12) shows the normalized $(dI/dV)/(I/V)$ vs V curves from the Ag-deposited Si(110)-(16 \times 2) surface. It is observed that the (16 \times 2) structures with an ultrathin layer of Ag on them now show a different electronic behavior. General features observed after Ag deposition in the normalized $(dI/dV)/(I/V)$ vs V spectra,

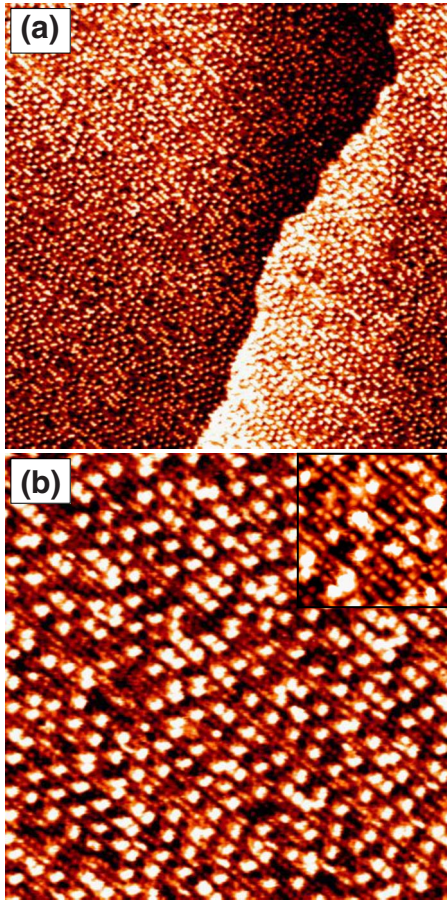


FIG. 7. (Color online) STM images of Si(110)-(5 \times 1) surfaces obtained following desorption of Ag deposited on a Si(110)-(16 \times 2) (coexisted with other reconstruction phases) surface. Scan area: (a) 200 \times 200 nm² and (b) 60 \times 60 nm². The inset in (b) represents a higher resolution STM image of the (5 \times 1) surface. The scan area of the inset in (b) is 15 \times 15 nm².

taken at different points on the upstripes and the downstripes of the (16 \times 2) structures, show the following features: (i) an increase in the band gap, (ii) band gap variation, (iii) band offset (shift of Fermi level, if Fermi level is defined to be at the middle of the band gap), and (iv) appearance of new electronic states within the band gap. We have investigated a theoretical model which provides a qualitative understanding of these observed features. This model is briefly discussed in Sec. IV and the details of this model are presented in the companion paper.

Although we mention band gap, which is taken to be the separation between the maximum in the LDOS at the highest energy in the filled states and the maximum in the LDOS at the lowest energy in the empty states, there may actually be low density of states between these energies. Before going to the presentation of the theoretical model, we present the results obtained after Ag desorption. As mentioned in Sec. II, upon Ag desorption, we do not get back the (16 \times 2) structure; only a (5 \times 1) reconstruction is observed (Fig. 7). This is consistent with previous observations that the presence of minute contamination leads to an absence of (16 \times 2) reconstruction and usually a (5 \times 1) reconstruction appears.¹⁵

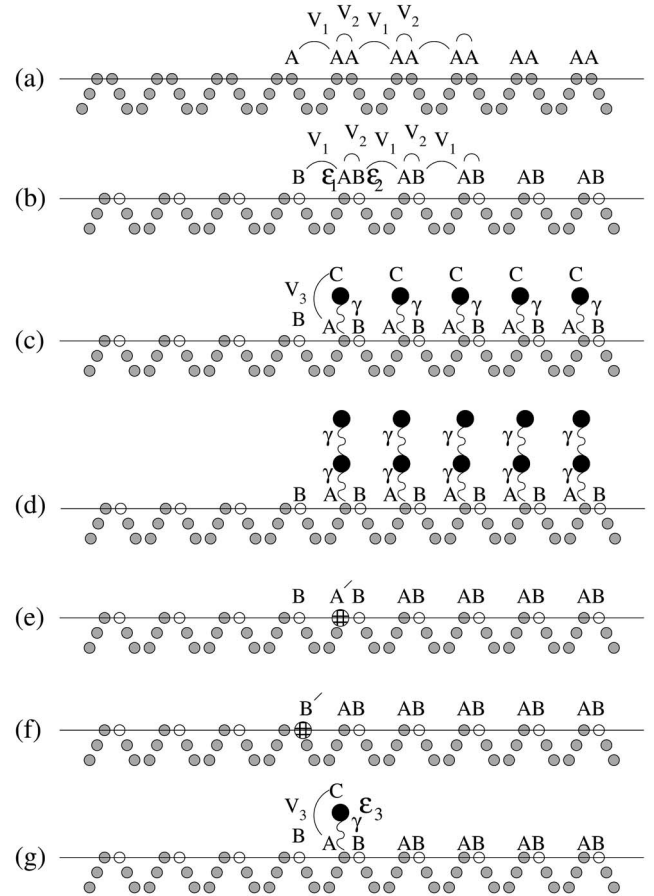


FIG. 8. A schematic model of the Si(110)-(16 \times 2) structures which represents different cases before Ag deposition (a) and after Ag deposition [(b)–(g)].

IV. THEORETICAL MODEL

Here, we briefly describe a theoretical model in order to understand the experimental results presented in the previous section. This model and its prediction are presented in detail in a companion paper. Here, we briefly discuss the main results obtained from the model. We construct a 1D model based on the Si(110)-(16 \times 2) reconstructed structure as follows: The (16 \times 2) structure with atomic arrangements is schematically shown in Fig. 2, which shows two upstripes and a unit cell is marked.¹⁵ As the separation between the stripes is \sim 5 nm, we assume this to be practically a 1D system and consider only one stripe, as shown in Fig. 8. We consider the atoms on the drawn line. The system is now like each atom having a long bond on one side and a short bond on the other side. Effectively this gives rise to two interaction parameters V_1 and V_2 . When the effect of other atoms below the line are taken into account, one would still expect to have two different interaction parameters instead of identical ones. In order to understand the band gap broadening and other observed phenomena after Ag deposition, we have performed a 1D tight binding model¹⁸ calculation to verify the local density of states and the associated increase in the band gap by using Green's function formalism.³ Considering different cases of the quasi-1D model, we discuss below as

to how this theoretical model can qualitatively explain our experimental data. A schematic diagram of the cases discussed is shown in Fig. 8.

The 1D structure is represented by the atoms on the line in Fig. 8. We notice that atoms A have two different A - A distances. They would have two interaction parameters V_1 (across the larger A - A distance) and V_2 (across the shorter A - A distance) and each A atom would have a site energy ε_1 .¹⁹ Figure 8(a) represents the case of two atoms per unit cell. The model leads to two bands with a band gap given by $|V_1 - V_2|$ and the width of each band is the smaller of $|V_1|$ and $|V_2|$. The details are given in the companion paper. Here, we briefly present the main results.

The band gap is given by

$$\Delta = |\alpha - \beta|, \quad (1)$$

where

$$\alpha = \frac{V_1}{V} \quad \text{and} \quad \beta = \frac{V_2}{V} \quad \text{with} \quad V = \frac{|V_1| + |V_2|}{2}.$$

If the alternating atoms are different, such as $ABAB\cdots$ [Fig. 8(b)], now there are two different site energies, ε_1 and ε_2 . The interaction parameters between short bond A - B and long bond A - B will still be different. However, keeping these values the same as V_1 and V_2 , as they are just parameters, the effect of site energy ε_2 becomes evident from the model. One now obtains a band gap widening and a shift of Fermi level.

The band gap is now given by

$$\Delta = \sqrt{\varepsilon^2 + (\alpha - \beta)^2}, \quad (2)$$

where

$$\varepsilon = \frac{\varepsilon_1 - \varepsilon_2}{2}$$

and the Fermi level is at

$$\varepsilon_F = \frac{\varepsilon_1 + \varepsilon_2}{2}. \quad (3)$$

Changing the second atom from A to B replaces the site energy ε_1 for the second atom to ε_2 . Thus, Eq. (3) indicates a shift of the Fermi level. The band gap broadening and Fermi level shift, observed in experiment (Fig. 6), are explained by Eqs. (2) and (3), respectively.

Next, we consider a modification of the case shown in Fig. 8(b). We consider that at every alternate lattice site, there is a dangling atom impurity (dangling bond) which repeats throughout the whole lattice. This introduces a new interaction energy γ [Fig. 8(c)]. This is the case of three atoms per unit cell. This case shows further widening of band gap and an associated Fermi level shift.

As the (16×2) reconstructed structure is not a purely one-dimensional system (Fig. 2) and there are interactions along the second dimension perpendicular to the nanowire-like structures, in order to mimic the effect of the second dimension in a limited way we consider the version of the model, as shown in Fig. 8(d). Here, a chain of two identical

dangling atoms is attached to every lattice site A . In this case there are four atoms per unit cell. This model gives further widening of band gap; however, it does not produce any additional Fermi level shift.

Finally, we consider the cases where a single A (or B) atom is replaced by an A' (or a B') atom, as shown in Fig. 8(e) [or Fig. 8(f)]. The presence of these (impurities) atoms introduces new electronic states within the band gap. The presence of single dangling atom, as shown in Fig. 8(g), also introduces a new electronic state within the band gap. These models offer a qualitative explanation of the observed states within the band gap (Fig. 6).

The variation of 1D tight binding model discussed above qualitatively explains the observed features in our STS results (Fig. 6), namely, (i) band gap widening, (ii) band gap variation, and (iii) band offset (Fermi level shift, if Fermi level is defined at the middle of the band gap), and the appearance of new electronic states within the band gap. This 1D tight binding model calculation using Green's function formalism is presented in details in a companion paper.

Our STS results (Fig. 6) were obtained from different locations on the nanowire-like stripes on the (16×2) structure following Ag deposition at room temperature. The spectra show a wide variation of band gap. Band gap widening can come from all the situations depicted in Figs. 8(b)–8(d). As we do not have a new ordered structure following Ag deposition, local variations in the electronic spectra are expected. We also observe considerable Fermi level shifts in the STS spectra (Fig. 6). As far as our theoretical model is concerned, two versions, as represented by Figs. 8(b) and 8(c), show Fermi level shift.

V. SUMMARY AND CONCLUSIONS

We have investigated the electronic structures of the Si(110)- (16×2) reconstructed surface and a low-coverage Ag-adsorbed Si(110)- (16×2) reconstructed surface by scanning tunneling spectroscopy. Electronic local density of states has been probed by the measurement of conductance. Local density of states on the nanowire-like stripes of Si on the (16×2) reconstructed bare Si(110) surface shows a band gap comparable to that for bulk Si. Upon low coverage ($\frac{1}{8}$ ML) Ag adsorption at room temperature on this surface, LDOS, in general, shows a wider band gap compared to bare surface. A variation of band gap has been observed when LDOS have been obtained from different spatial locations. If the Fermi level of the system is defined at the middle of the band gap, then a variation of the position of the Fermi level has been observed. In addition, new electronic states appear within the band gap. All these features are qualitatively explained by the one-dimensional tight binding model using Green's function formalism. Many features of similar problems can be investigated by this model. For example, the effect of various types of sequences in the dangling or side chains can be investigated. Though not investigated here, the effect of length disorder of the side chain on the spectra can also be investigated.

*bhupen@iopb.res.in; msbnd@iacs.res.in

- ¹M. Menon, N. N. Lathiotakis, and A. N. Andriotis, *Phys. Rev. B* **56**, 1412 (1997).
- ²A. A. Stekolnikov, J. Furthmuller, and F. Bechstedt, *Phys. Rev. B* **70**, 045305 (2004).
- ³*Green's Functions in Quantum Physics*, by E. N. Economou, 2nd ed. (Springer-Verlag, Berlin, 1983); M. Kohmoto, B. Sutherland, and C. Tang, *Phys. Rev. B* **35**, 1020 (1987).
- ⁴Samar Chattopadhyay, Ph.D. thesis, University of Kalyani, 2005.
- ⁵H. Ampo, S. Miura, K. Kato, Y. Ohkawa, and A. Tamura, *Phys. Rev. B* **34**, 2329 (1986).
- ⁶Y. Yamamoto, *Phys. Rev. B* **50**, 8534 (1994).
- ⁷Y. Yamamoto, T. Sueyoshi, T. Sato, and M. Iwatsuki, *Surf. Sci.* **466**, 183 (2000).
- ⁸T. An, M. Yoshimura, I. Ono, and K. Ueda, *Phys. Rev. B* **61**, 3006 (2000).
- ⁹B. A. Nesterenko, A. V. Brovii, and A. T. Sorokovykh, *Surf. Sci.* **171**, 495 (1986).
- ¹⁰E. J. van Loenen, D. Dijkkamp, and A. J. Hoeven, *J. Microsc.* **152**, 487 (1988).
- ¹¹T. Ichinokawa, H. Ampo, S. Miura, and A. Tamura, *Phys. Rev. B* **31**, 5183 (1985).
- ¹²Y. Yamamoto, S. Ino, and T. Ichikawa, *Jpn. J. Appl. Phys., Part 2* **25**, L331 (1986).
- ¹³A. Cricenti, P. Perfetti, B. Nesterenko, G. LeLay, and C. Sebenne, *J. Electron Spectrosc. Relat. Phenom.* **76**, 481 (1995).
- ¹⁴A. Cricenti, B. Nesterenko, P. Perfetti, G. LeLay, and C. Sebenne, *J. Vac. Sci. Technol. A* **14**, 2448 (1996).
- ¹⁵W. E. Packard and J. D. Dow, *Phys. Rev. B* **55**, 15643 (1997).
- ¹⁶A. A. Stekolnikov, J. Furthmuller, and F. Bechstedt, *Phys. Rev. Lett.* **93**, 136104 (2004).
- ¹⁷D. K. Goswami, B. Satpati, P. V. Satyam, and B. N. Dev, *Curr. Sci.* **84**, 903 (2003).
- ¹⁸P. K. Datta, D. Giri, and K. Kundu, *Phys. Rev. B* **47**, 10727 (1993); K. Kundu, D. Giri, and K. Ray, *J. Phys. A* **29**, 5699 (1996).
- ¹⁹D. H. Dunlap, H. L. Wu, and P. W. Phillips, *Phys. Rev. Lett.* **65**, 88 (1990).